Journal of Applied Polymer Science

Preparation of polypropylene/octadecane composite films and their use in the packaging of cherry tomatoes

Dowan Kim, Mijin Lim, Jongchul Seo
Department of Packaging, Yonsei University, 1 Yonseidae-Gil, Wonju, Gangwon-Do 220-710, Korea
Correspondence to: J. Seo (E-mail: jcseo@yonsei.ac.kr)

ABSTRACT: Polypropylene (PP)/octadecane (OD) composite films were prepared via twin-screw extrusion, and their chemical, morphological, thermal, and surface properties and oxygen and water vapor permeabilities were analyzed as functions of the OD content and temperature. OD was dispersed well in the PP matrix, and two phases (i.e., the PP and OD portions) were present in the PP/OD composite films. When the temperature was increased from 10 to 30 °C, both the oxygen transmittance rate and the water vapor transmittance rate of the PP/OD composite films increased sharply because of the influence of the OD content. These results were related to the temperature-dependent changes in the morphological structure, such as changes in the the tortuous paths and crystallinity in the composite films because of the addition of OD. In the storage test, the PP/OD (83:17) composite films continuously controlled the gas concentration of the headspace and protected against environmental factors; this reduced the enzymatic activity and led to higher quality cherry tomatoes compared to the case when the pure PP and MP33000 films were used. © 2016 Wiley Periodicals, Inc. J. Appl. Polym. Sci. **2016**, *133*, 44087.

KEYWORDS: composites; functionalization of polymers; packaging; phase behavior; stimuli-sensitive polymers

Received 12 February 2016; accepted 13 June 2016
DOI: 10.1002/app.44087

INTRODUCTION

Temperature plays a significant role in maintaining the quality and extending the shelf life of agricultural products during shipping, storage, and sales.[1–6] In general, a low-temperature environment can extend the shelf life by reducing the respiration rate of agricultural products, the growth rate of microorganisms, and various physical and chemical reactions that occur in agricultural products.[3,5,6] A drastic rise in the temperature increases the respiratory rate of agricultural products; this leads to the fast consumption of O_2 and the generation of high levels of water vapor and CO_2 in the packaging.[3,5,6] As a result, physiological changes, such as an increase or decrease in brix, color changes, rancidity, hardening or softening of texture, and microbial and fungal spoilage, of agricultural products occur easily.

To control the respiration rate of agricultural products, modified atmosphere packaging systems have been widely studied.[5,6] Modified atmosphere packaging is an active packaging system that uses a gas-exchange membrane to maintain adequate concentrations of gases, typically O_2, water vapor, and CO_2, for the prolonged freshness of packaged products.[3,4,6] In general, the modified atmosphere inside the packaging relies on several factors, including the permeability of the packaging materials, respiration rate of the products, and headspace.[7,8] To enhance and control the permeability of packaging materials, many recent studies have focused on perforation methods with cold or hot needles and microelectric discharge machining.[7,8] Perforation methods for packaging materials are an alternative approach for controlling the respiration rate of agricultural products; however, the respiration rate depends strongly on the temperature and the permeability of the packaging materials.[6,9] In addition, there are still drawbacks, such as attacks from microorganisms during postharvest handling, the risk of moisture permeation in the product, a loss of flavors in the product, and a loss of mechanical properties, when the products are packaged with perforated films.[7] Although unwanted temperature changes occur continuously during shipping and storage, conventional packaging materials, including perforated films, cannot cope well with the permeability and changes in temperature because of their poor insulation and low thermal buffering capacity.[3,6,9] Therefore, a sustainable balance between the respiration rate of products and the gas permeation in packaging materials are necessary to handle unwanted temperature changes. To solve these problems, researchers have investigated polymers with temperature-dependent gas permeabilities, including (1) side-chain crystallizable polymers based on *n*-alkyl acrylate,[6,9] (2) poly(*N*-isopropyl acrylamide) hydrogels,[2,4] and (3) polyurethane with a thermally reversible soft segment and a fixed phase (hard segment).[5]

Table I. Compositions of the PP/OD Composite Films

Composition	PP (g)	OD (g)	Total (g)
Pure PP	300	0	300
PP/OD (95:5)	300	15	315
PP/OD (91:9)	300	30	330
PP/OD (83:17)	300	60	360

The introduction of phase-change materials (PCMs) into polymer matrices is one possible approach for minimizing the negative effects of unwanted temperature changes.[3,10,11] PCMs are materials that absorb and release large amounts of latent heat energy during temperature-driven phase changes, such as melting and crystallization.[12] PCMs with a low molecular weight, such as tetradecane, octadecane (OD), and paraffin wax (PW), cannot be used without a container, such as an inorganic filler or a polymer matrix, because of the inevitable lack of shape stability and incongruent thermal behavior during solid–liquid phase-change process.[10–13] There are many reports on the preparation and characterization of polymer and PCM composites for the sustainable and safe use of PCMs.[1–4,12,14,15] In our previous study, low-density polyethylene (LDPE)/PW composite films were fabricated, and their temperature-dependent oxygen and water vapor permeations were analyzed as functions of the PW content. The crystallinity of PW in LDPE decreases rapidly, and the chain mobility of PW in the LDPE matrix increases when the temperature is increased close to the phase-change temperature of PW.[3] As a result, LDPE/PW composite films seem to open permeation channels effectively for gas molecules in the polymer matrix over the range of the phase-change temperature.[3]

OD has a large latent heat-storage capacity and a phase-change temperature around 26–29 °C and is nontoxic and readily available.[12] To ensure a stable and long-term thermal and permeability performance of PCM in the polymer matrix, we prepared polypropylene (PP)/OD composite films with a reversible phase transition. PP/OD composite films were prepared with a twin-screw extruder, and their morphology and physical properties, including their oxygen permeability and water permeability, were thoroughly investigated as a function of the OD content. Finally, changes in the O_2 and CO_2 concentrations inside packaging for cherry tomatoes with PP/OD composite films were analyzed, and their effects on the firmness and color of the cherry tomatoes were monitored over 15 days at 9 and 23 °C.

EXPERIMENTAL

Materials

For the matrix polymer, FC-150U homo PP resin was provided by Lotte Chemical Co., Ltd. (Seoul, Korea). PP had a melt flow index of 8 g/10 min (ASTM D 1238), a molecular weight of 250,000–300,000 g/mol, and a density of 0.90 g/cm^3. For the PCM, OD with a density of 0.78 g/cm^3 and a melting point of 26–29 °C was purchased from Sigma Aldrich Co., Ltd. (Yongin, Korea). All of the materials in this study were used without further purification. Cherry tomatoes were purchased from E-Mart (Wonju, Korea).

Preparation of the PP/OD Composite Films

Four different PP/OD composite compounding pellets were prepared with a twin-screw extruder (BA-19, BauTech Co., Uijeongbu, Korea) with a length/diameter ratio of 40:19 according to the compositions listed in Table I. To remove the water in the compounding pellets, the pellets were dried in a drying oven at 80 °C for 12 h. With the as-prepared pellets, four different PP/OD composite films were prepared with a twin-screw extruder. The extruder was equipped with a switchable header with an orifice for making pellets and a T-die for making films. The extruder was set to 190 °C for the header, 190 °C for zones 1–6, and 120 °C for the feed zone. The thickness of the composite films was maintained at approximately 65 ± 2 μm.

Packaging of the Cherry Tomatoes

Six cherry tomatoes with a total weight of 72.8 ± 1.5 g were placed in PP trays (15 cm in length × 12 cm in width × 5 cm in depth), and the trays were heat-sealed with three different films (pure PP film, PP/OD (83:17) composite film, and microperforated PP film [MP33000; oxygen transmission rate (OTR) = 32,244 and 33,098 cc/m^2·day at 10 and 23 °C] with an impulse sealing machine (model ISS 350-5, Gasungpak Co., Ltd., Gwangju, Korea). A commercial MP33000 film was kindly supplied from Our Home Co., Ltd. (Seoul, Korea). Cherry tomato trays packaged with the three different films were stored in temperature-controlled chambers at 9 and 23 °C. Five packages were used for each day of analysis.

Characterization

To analyze the chemical and/or physical interactions between PP and OD in the composite films, Fourier transform infrared (FTIR) spectra were obtained with a Spectrum 65 FTIR spectrometer (PerkinElmer Co., Ltd., Waltham, MA) from 400 to 4000 cm^{-1} with the attenuated total reflection mode.

To identify the dispersion and miscibility state of OD in the PP matrix, images of the fractured surface were obtained with a

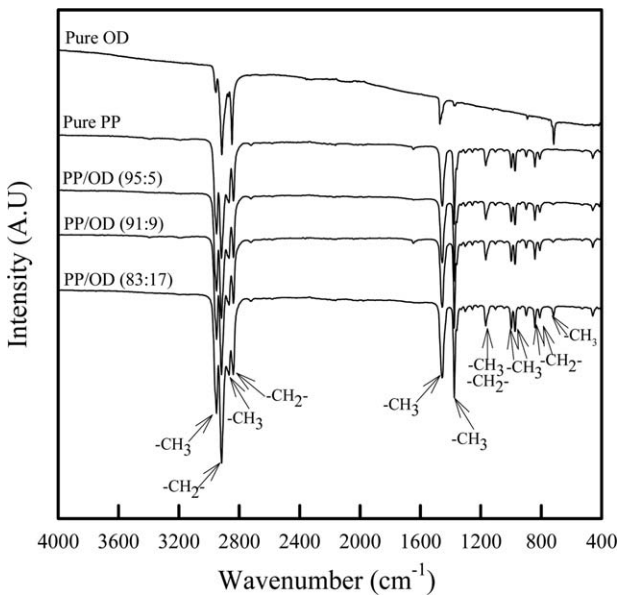

Figure 1. FTIR spectra of the pure OD, pure PP, and PP/OD composite films.

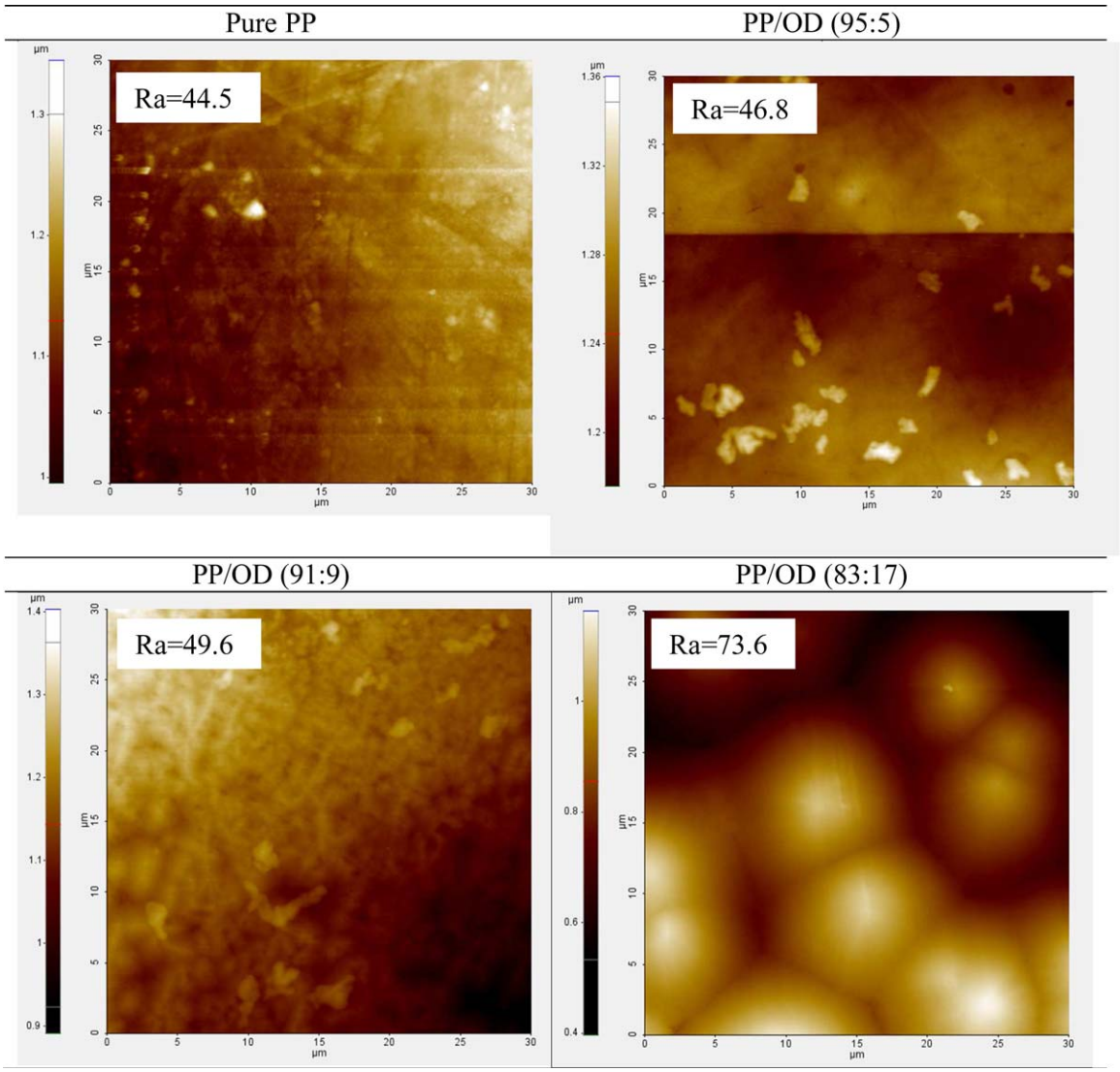

Figure 2. AFM images of the top surfaces of the pure PP and PP/OD composite films. Ra, roughness average. [Color figure can be viewed in the online issue, which is available at wileyonlinelibrary.com.]

Quanta FEG250 scanning electron microscope (FEI Co., Ltd., Hillsboro, OR). Before the examination, the composite films were coated with a thin layer of Pt/Pd. In addition, miscibility and roughness studies on the PP/OD composite films were performed with an NX 10 atomic force microscope (Park System Co., Ltd., Suwon, Korea). Quantitative analysis in the height mode was performed with XEI software. All atomic force microscopy (AFM) measurements were performed in noncontact mode with a silicon nitride tip at ambient temperature in an air atmosphere.

Differential scanning calorimetry (DSC) of the composite films was conducted with a Q10 differential scanning calorimeter (TA Instrument Co., Ltd., New Castle, DE) in a nitrogen atmosphere. The samples were heated from −50 to 200 °C at a rate of 10 °C/min. The melting and crystallization temperatures and the enthalpies of the composite films were calculated with the TA universal analysis software (TA Instrument). The percentage crystallinity of the PP/OD composite films was calculated with eq. (1):

$$\text{Percentage crystallinity} = \Delta H_m / \Delta H_m^o \times 100 \quad (1)$$

where ΔH_m is the melting enthalpy of the composite films and ΔH_m^o is the melting enthalpy of the fully crystalline PP sample (209 J/g).[16]

To determine the thermal stability of the OD, PP, and PP/OD composite films, thermogravimetric analysis (TGA) was performed with a TGA 4000 thermogravimetric analyzer (PerkinElmer Co., Ltd., Waltham, MA) at a heating rate of 10 °C/min from 50 to 700 °C in nitrogen.

The OTRs of the PP/OD composite films were measured with an OTR 8001 oxygen permeability tester (Systech Instruments Co., Ltd., Johnsburg, IL). To investigate the effect of the temperature on the permeabilities, OTR tests was performed at 5, 10, 15, 23, 26.5, 38, and 48 °C. The water vapor transmission rates (WVTRs) of the PP/OD composite films were measured with a Mocon Permatran-W 3/33 (Mocon, Inc., Minneapolis, MN). To investigate the effect of the temperature on the permeabilities,

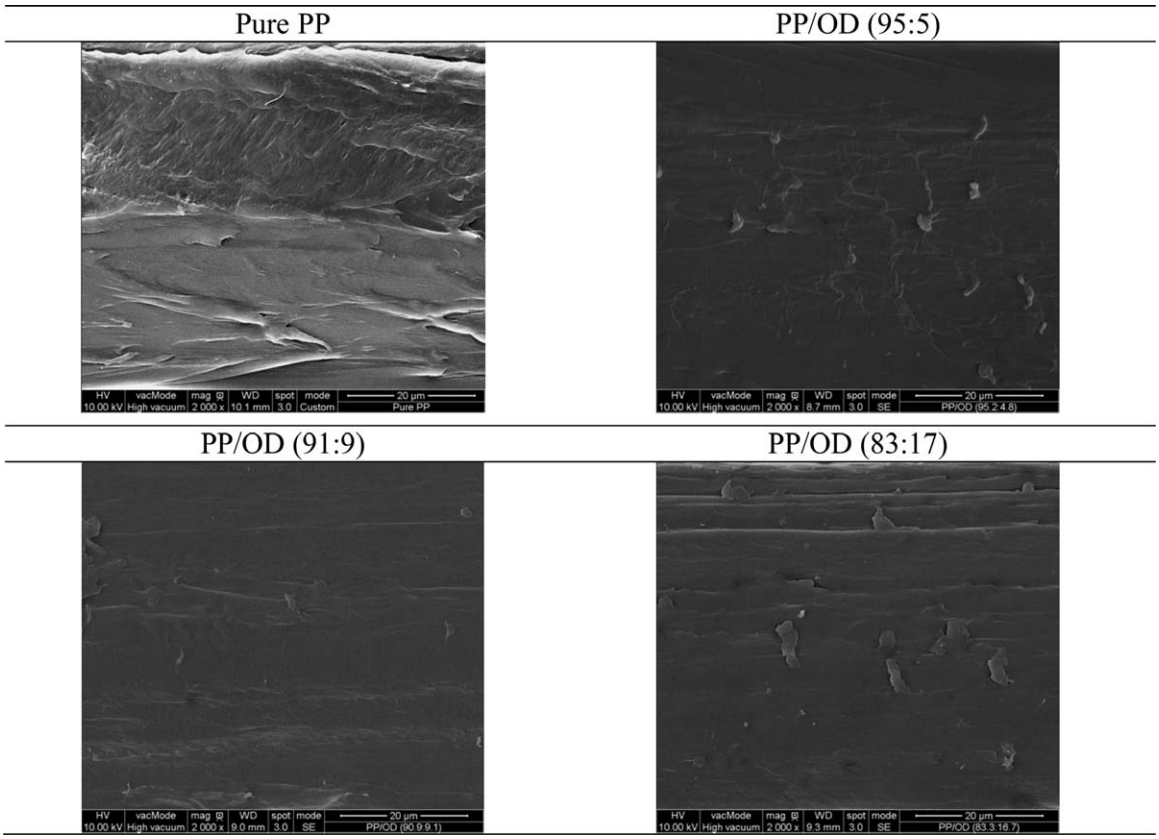

Figure 3. SEM images of the fractured surfaces in the pure PP and PP/OD composite films.

WVTR tests were performed at 10, 15, 23, 26.5, 38, and 48 °C. The oxygen and water vapor permeability experiments were repeated in triplicate.

The contact angles and surface properties of the PP/OD composite films were investigated with a Phoenix 300 contact angle goniometer (SEO Co., Ltd., Suwon, Korea). The surface free energies (γ^ss) of the PP/OD composite films were estimated via the Owens–Wendt geometric mean equation with the theory of adhesion between films and liquid;[3,17] that is, the γ^s values could be calculated by the addition of the polar energy (γ^P) and nonpolar or dispersive energies (γ^D).[3,17] Polar water ($\gamma^s = 72.8$ mJ/m^2, $\gamma^P = 51.0$ mJ/m^2, $\gamma^D = 21.8$ mJ/m^2) and nonpolar diiodomethane ($\gamma^s = 50.8$ mJ/m^2, $\gamma^P = 50.4$ mJ/m^2, $\gamma^D = 0.4$ mJ/m^2) were used as proving liquids. Furthermore, the solubility parameter (δ), an indicator of the hydrophilicity or hydrophobicity of a polymer surface, was calculated with eq. (2)[3,18,19]:

$$\delta = (e_{\mathrm{coh}})^{1/2}, \tag{2}$$

where e_{coh} is the cohesive energy density of the materials used, such as the OD, PP, and PP/OD composite films, and can be calculated with eq. (3)[3,18,19]:

$$\gamma^s = 0.75(e_{coh})^{2/3}. \tag{3}$$

The O_2 and CO_2 compositions of the headspace of the cherry tomato trays packaged with the pure PP film, PP/OD (83:17) composite film, and MP33000 were investigated with an O_2/CO_2 gas analyzer (PBI-Densenor, Inc., Ringsted, Denmark) through insertion of the needle of the measuring apparatus through a septum adhered to the sealed films.[20,21] The firmness of the cherry tomatoes in the packaging was measured with a fruit hardness tester FR-5105 (Lutron Electronic Enterprise Co., Ltd., Taipei, Taiwan). A rod 3 mm in diameter was placed perpendicular to the surface and pressed on the cherry tomato.[22] The surface color of the cherry tomatoes was measured with a TES 135A colorimeter (TES Electrical Electronic Co., Ltd., Taipei, Taiwan).[22]

RESULTS AND DISCUSSION

Preparation of the PP/OD Composite Films

FTIR analysis was performed to confirm the chemical structure and interfacial interactions between OD and PP, as shown in Figure 1. Despite the similar chemical structure of PP and OD, PP showed complex characteristic peaks because of various stretching, deformation, wagging, and rocking vibrations originating both from its high molecular weight and —CH_3 pendent groups, compared to the low-molecular-weight OD[23,24]: —CH_3 asymmetric stretching vibrations at 2950 cm^{-1}, symmetric stretching vibrations at 2838 and 2918 cm^{-1} due to —CH_2— and at 2868 cm^{-1} due to —CH_3, an asymmetric deformation vibration at 1454 due to —CH_3, a symmetric deformation vibration at 1376 due to —CH_3, carbon lattice pulsation at 1302 and 1256 cm^{-1}, wagging and deformation vibration at 1166 cm^{-1} due to —CH_3 and —CH_2—, and rocking vibrations at 998 and 974 cm^{-1} due to —CH_3 and 842 and 808 cm^{-1} due to —CH_2—.[23,24] The intensity of the absorption bands at 717 cm^{-1} implied that the in-plane rocking vibrations of —CH_3 gradually

Table II. Thermal Properties of the OD and PP/OD Composite Films

	DSC									TGA		
Sample code	T_{m1} (°C)[a]	T_{m2} (°C)[b]	ΔH_{m1} (J/g)[c]	ΔH_{m2} (J/g)[d]	ΔH_{total} (J/g)[e]	T_{c1} (°C)[f]	T_{c2} (°C)[g]	ΔH_{c1} (J/g)[h]	ΔH_{c2} (J/g)[i]	X_c	$T_{d1\%}$ (°C)[k]	$T_{d3\%}$ (°C)[k]	Weight loss (wt %)[l]
OD	29.6	—	220.0	—	—	26.2	—	218.4	—	—	135.1	179.1	—
Pure PP	—	166.1	—	94.7	94.7	—	115.2	—	92.8	45.3	341.4	366.1	—
PP/OD (95:5)	4.4	163.3	2.7	96.8	99.5	−10.3	112.6	2.9	96.1	47.6	180.4	231.6	6.6
PP/OD (91:9)	6.2	162.9	4.7	103.6	108.3	−9.0	113.9	4.3	103.8	51.8	160.6	212.4	8.4
PP/OD (83:17)	17.9	161.5	13.5	81.5	95.0	7.3	109.4	14.0	80.3	45.5	146.5	179.8	13.6

X_c, crystallinity of the PP/OD composite films.
[a,b] T_{m1} and T_{m2} of the OD and PP/OD composite films, respectively.
[c,d] ΔH_{m1} and ΔH_{m2}, melting enthalpies of the OD and PP/OD composite films, respectively.
[e] $\Delta H_{m,total}$, total melting enthalpy of PP/OD composite films.
[f,g] T_{c1} and T_{c2}, crystallization temperatures of the OD and PP/OD composite films, respectively.
[h,i] ΔH_{c1} and ΔH_{c2}, crystallization enthalpies of OD and PP/OD composite films, respectively.
[k] $T_{d1\%}$ and $T_{d3\%}$, 1 and 3% decomposition temperatures, respectively, of the OD and PP/OD composite films.
[l] Weight loss of OD content in the PP/OD composite films at 340 °C.

increased with the OD content in the composite films.[25,26] The PP/OD composite films showed characteristic peak positions similar to those of pure PP; this may have occurred because the majority of the characteristic peaks between PP and OD overlapped because of their similar chemical structure.[3,23–26] In addition, the density of the alkyl chains attached to PP was higher than that of OD; this prevented chain mobility of the asymmetric and symmetric stretching bands and the in-plane rocking vibration band.[3,23,24]

Morphology of the Composite Films

As shown in Figures 2 and 3, AFM and scanning electron microscopy (SEM) analyses were performed to investigate the dispersion state and miscibility of OD in the PP matrix.[3,13,27] As shown in Figure 2, the pure PP showed a relatively smooth and uniform top surface. When the OD content in the PP matrix increased, the OD dispersed well in the PP matrix, and the top surfaces of the PP/OD composite films grew rougher; this produced micrometer-sized crystals of different shapes originating from the different molecular weights. According to the results, two different phases existed in the PP/OD composite films, that is, a temperature-dependent reversible OD phase and a relatively immobile PP phase. The OD phase may act as a temperature-dependent permeation path for oxygen and water vapor molecules when the temperature increased from 10 to 30 °C. In the fractured surface (Figure 3), there were no cracks or voids observed inside. This finding indicated that good adhesion and interfacial interaction between the nonpolar OD and nonpolar PP were maintained to some degree.[13]

Thermal Properties

As shown in Figure 4 and Table II, the degradation patterns and thermal stability depended on the OD content. The flash point and boiling point of OD were 166 and 317 °C, respectively.[28–30] During thermal degradation, pure PP showed a one-step degradation process, and the structural decomposition of pure PP started at 341 °C ($T_{d1\%}$). This degradation stage was due to the decomposition of the propylene trimer in PP.[31] All of the PP/OD composite films exhibited a two-step degradation process with the addition of different OD concentrations. The first degradation stage between 130 and 340 °C was because of decomposition near the flash temperature of OD[28,29] or evaporation before the boiling temperature of OD,[28,30] and the second stage (340–480 °C) was a chemical degradation process resulting from bond scission and chain-transfer reactions in the pure PP.[32]

The weight loss (6.6, 8.4, and 13.6%) because of the OD content in the composite films at 340 °C was slightly different from those calculated theoretically (4.7, 9.0, and 16.7%). These results indicate that OD with a low thermal stability was successfully incorporated into the PP matrix at low OD concentrations. However, some evaporation occurred during the extrusion process; that is, the weight loss of the composite films over the range 200–400 °C was attributed to OD, which had much shorter chains and was less thermally stable than pure PP. On the basis of the thermal stabilities of the PP/OD composite films, we speculated that further surface modifications were needed to enhance the interfacial interaction and thermal

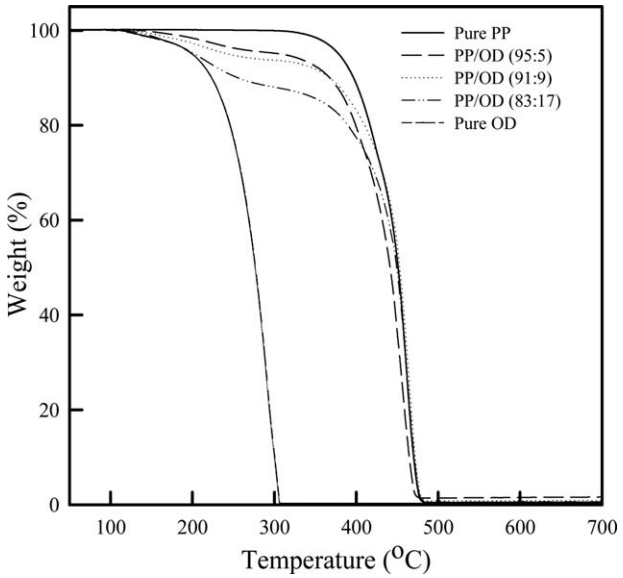

Figure 4. TGA curves for the PP/OD composite films.

stability between PP and OD to perform the extrusion process at high pressure and temperature.

An understanding of the thermal properties is required to design polymer structures with temperature-dependent oxygen and water vapor permeabilities.[33–35] On the basis of Figure 5 and Table II, we surmised how the OD content affected the morphological structure, such as the amorphous and crystalline structure, in the pure PP matrix.

According to Figure 5(a), the pure OD showed a sharp endothermic peak at 29.6 °C during heating and an exothermic peak at 26.2 °C during cooling. These peaks were related to the solid–liquid (melting) transition and liquid–solid (solidification) transition, respectively.[13] ΔH_m and the crystallization enthalpy (ΔH_c) of the pure OD were calculated to be 220.0 and 218.4 J/g, respectively. As shown in Figure 5(b), the pure PP exhibited one endothermic peak at 166.1 °C during heating and one exothermic peak at 115.2 °C during cooling. New melting and crystallization enthalpy values based on the crystalline phases of the OD portion [initial melting temperature (T_{m1}) and initial crystallization temperature (T_{c1})] increased from 2.7 to 13.5 J/g and from 2.9 to 14.0 J/g, respectively, as the OD content was increased up to 16.7%. In addition, the melting and crystallization enthalpy values based on the crystalline phases of the PP portion [second melting temperature (T_{m2}) and second crystallization temperature (T_{c2})] increased with the addition of up to 9.1% OD. However, the PP/OD (83:17) composite film did not exhibit a noticeable increase. According to the results, the PP/OD composite films showed two endothermic peaks; this implied independent crystallization of the components (i.e., OD and PP). That is, the number of new crystallites originating from OD entering the PP lattice increased; this caused a change in the morphological structure of the composite films.

In addition, T_{m1} and T_{c1} in the composite films increased from 4.4 to 17.9 °C and from −10.3 to 7.3 °C, respectively, and T_{m2} and T_{c2} decreased from 166.1 to 161.5 °C and from 115.2 to 109.4 °C, respectively. This result shows that the melting temperatures (T_{m1} and T_{m2}) and crystallization temperatures (T_{c1} and T_{c2}) were lower than those of OD and PP. This result may have been related to the miscibility between PP and OD in the molten state; this partially altered the crystal formation and led to the formation of small crystallites of OD and PP in the composite films.[3,34]

According to our results, OD altered the morphological structure of the PP matrix. OD caused a significant temperature dependence of the amorphous and crystalline structure in the composite films. As the temperature increased to near T_{m1} (10–30 °C), the crystalline structure of OD started to disentangle and rearrange in the PP matrix. At a low concentration of OD in the PP matrix, PP interacted relatively well with OD. This predominantly affected the chain mobility and the crystalline

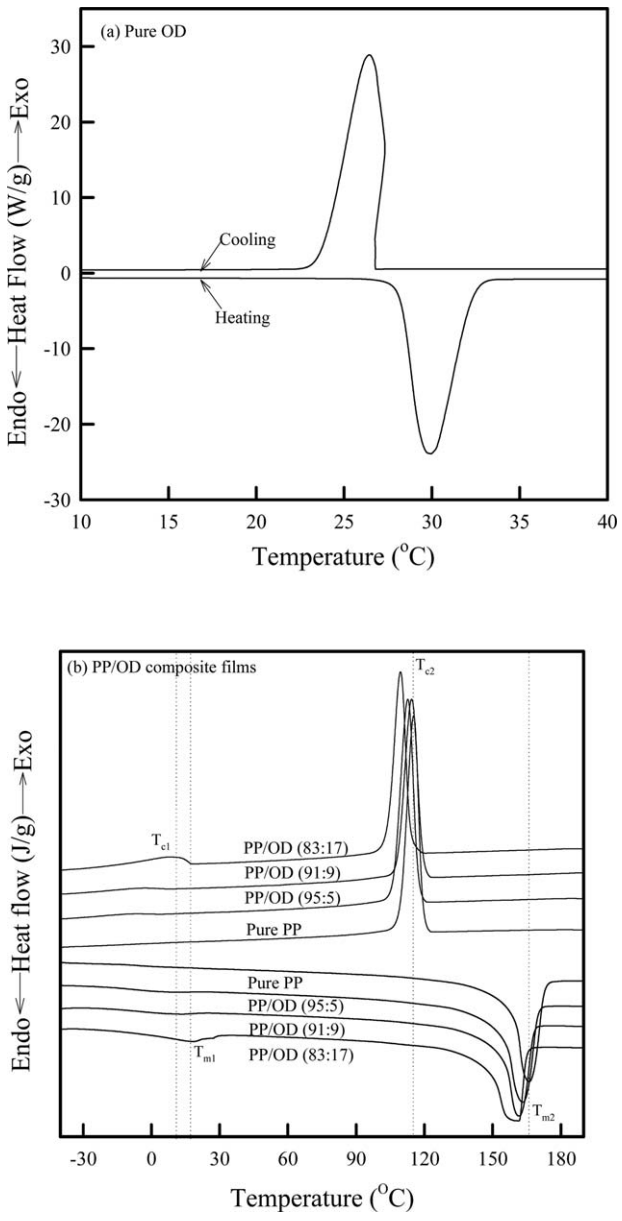

Figure 5. DSC curves for the (a) OD and (b) PP/OD composite films.

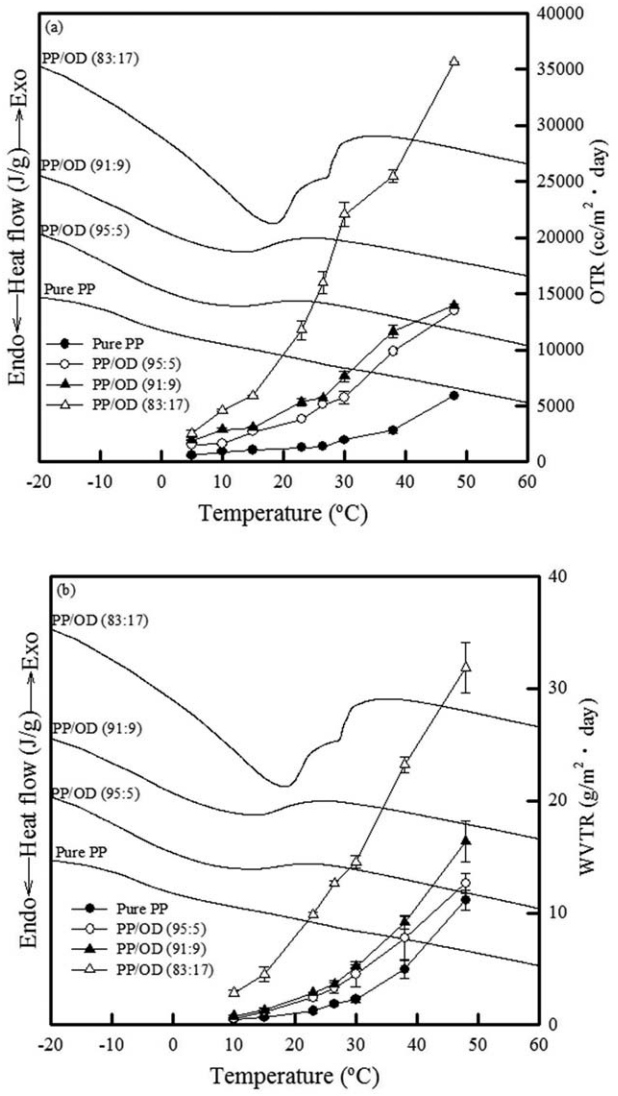

Figure 6. (a) OTR and (b) WVTR curves for the PP/OD composite films.

structure in the composite films and might have impeded the disentanglement and rearrangement of OD in PP. At a high OD content (16.7%), however, OD easily collapsed from a crystalline structure to an amorphous structure during the phase-change process because of the decreased crystalline structure of PP.

Oxygen and Water Vapor Permeabilities

Figure 6 shows the oxygen and water vapor permeabilities of the PP/OD composite films based on the DSC analysis. The OTR of pure PP varied linearly from 586 to 5897 cc/m^2·day as a function of temperature from 5 to 48 °C. As the OD content increased in the PP matrix, the OTR of the PP/OD composite films dramatically increased from 1540 to 13 428, from 1948 to 13 967, and from 2524 to 35 607 cc/m^2·day. The WVTR results exhibited a similar trend as those of the OTR results. The WVTR of the pure PP film increased from 0.5 to 11.1 g/m^2·day, whereas the WVTR of the PP/OD composite films increased from 0.6 to 12.6, from 0.8 to 16.3, and from 2.9 to 31.9 g/m^2·day with a temperature increase from 10 to 48 °C. In general, the oxygen and water vapor permeabilities increase significantly with temperature according to the Arrhenius equation.[6,9] In our studies, the magnitude of the increase in the permeation for oxygen and water vapor started to increase between 10 and 30 °C as the OD content in PP increased. To interpret the permeation jump, we used the modified two-phase model proposed by Michaels and Bixler,[6,9,36,37] as described by eq. (4):

$$P_c = P_a(1-\Phi)/\tau\beta, \quad (4)$$

where P_c is the permeability of the composite film with a semicrystalline structure, P_a is the completely amorphous structure in the composite films, Φ is the volume fraction of the crystalline structure, τ is a tortuosity factor, and β is the immobilization of the amorphous structure because of the existence of the crystalline structure.[6,9,36,37] We assumed that the crystalline structure was less permeable to penetrants such as oxygen and water vapor molecules, and this led to a tortuous path for permeation.[6,9,36,37] However, the penetrants easily passed through the amorphous structure in the composite films.[6,9,36,37] Thus, the model suggested that the gas permeability in the polymer depended strongly on the amorphous and crystalline structure. In this study, OD served as the new crystalline structure in the PP matrix. When the temperature increased from 10 to 30 °C, the crystalline structure of OD started to become amorphous, and this caused an increase in the chain mobility induced by OD in the PP matrix, as described by the DSC analyses. At a low concentration of OD, however, the permeation increase was weakened because the crystalline structure of PP hindered the morphological change from a crystalline structure to an amorphous structure with temperature. As the OD content increased, it strongly affected the morphological structure of the PP/OD composite films. During the phase-change process of OD, the intramolecular interactions in OD collapsed; this contributed to a decrease in the volume fraction of the crystalline structure, which weakened the immobilization of the amorphous structure because of the presence of the crystalline structure in the PP/OD composite films. As a result, the composite films seemed to open permeation paths for oxygen and water vapor.

The surface properties, including the degrees of hydrophobicity and hydrophilicity, and the δ of the composite films were significant because of their important relationship with the oxygen and water vapor permeabilities.[3,17,38] The contact angle of different liquids such as water, which is polar, and diiodomethane, which is nonpolar, on the polymer can provide important information to interpret their physical and chemical interactions. As shown in Figure 7 and Table III, the water and diiodomethane contact angles for the pure nonpolar OD were 100.7 and 27.9°, respectively. The pure PP, which was nonpolar, exhibited water and diiodomethane contact angles of 95.1 and 48.0°, respectively. OD had shorter chains than PP and could be easily absorbed in the nonpolar diiodomethane, although they had similar chemical structures.

The PP/OD composite films showed increased water contact angles from 95.1 to 101.2°, whereas the diiodomethane contact angles of the PP/OD composite films decreased slightly from 48.0 to 43.4° with up to 16.7% OD loading in the PP matrix.

Table III. Contact Angle, γ^s, e_{coh}, and δ Values of the Pure OD, Pure PP, and PP/OD Composite Films

	Contact angle (°)		γ^s (mJ/m^2)				
Sample code	Water	Diiodomethane	Total	Dispersive	Polar	e_{coh} (10^6 J/m3)	δ (10^3 J$^{1/2}$/m$^{3/2}$)
OD	100.7	27.9	45.4	45.4	0.0	471.0	21.7
Pure PP	95.1	48.0	35.2	34.6	0.6	321.5	17.9
PP/OD (95:5)	97.5	43.6	37.5	37.3	0.2	353.6	18.8
PP/OD (91:9)	98.4	43.6	37.5	37.4	0.1	353.6	18.8
PP/OD (83:17)	101.2	43.4	37.8	37. 8	0.0	357.8	18.9

This result indicates that the hydrophobicity of the PP/OD composite films increased slightly, and the potential interaction of the nonpolar liquid with the PP/OD composite films increased as the OD content increased. In general, γ^s generally decreases when the hydrophobicity increases.[3,17,38] However, our results showed the opposite trend. As shown in Figure 7, OD, which had nonpolar functional groups such as —CH_2— and —CH_3, showed γ^s values of 0.0 mJ/m^2 for the polar part and 45.4 mJ/m^2 for the dispersive part. The γ^s values of the polar and dispersive parts in the pure PP were 0.6 and 34.6 mJ/m^2, respectively. The polar part of the γ^s of the PP/OD composite films decreased slightly from 0.6 to 0.0 mJ/m^2. The γ^s of the dispersive part, which was related to the surface roughness and nonpolarity, increased slightly from 34.6 to 37.8 mJ/m^2. Finally, the total γ^s of the composite films increased slightly from 35.2 to 37.8 mJ/m^2 with an increase in the OD content of the PP matrix. These results show trends similar to those of δ. δ was 17.9×10^3 J$^{1/2}$/m$^{3/2}$ for the pure PP and varied slightly from 17.9×10^3 to 18.9×10^3 J$^{1/2}$/m$^{3/2}$ for the PP/OD composite films. δ of water was 47.9×10^3 J$^{1/2}$/m$^{3/2}$.[3,18] Thus, the difference in the δs between the composite films and water decreased slightly with the addition of OD to PP; this indicated that water vapor could be easily absorbed and could diffuse into the PP/OD composite films.

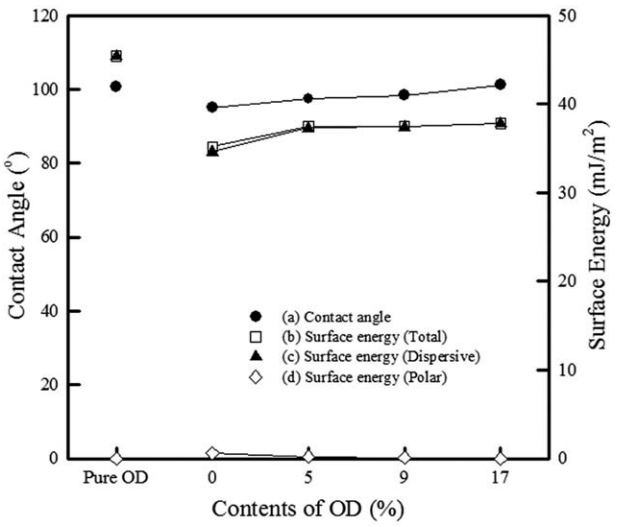

Figure 7. Contact angles and γ^s values of the pure OD, pure PP, and PP/OD composite films.

Storage Test with Cherry Tomatoes

The headspace atmosphere of packaged cherry tomatoes is strongly affected by the storage temperature and gas transmission rate of the packaging materials.[20,21] As shown in Figure 8, packaged cherry tomatoes with the pure PP films experienced a depletion of O_2 (1.6%) and an accumulation of CO_2 (2.8%) over 15 days of storage at 9 °C. The PP/OD (83:17) composite film and MP33000 film maintained similar concentration levels of O_2 and CO_2 compared to the pure PP. When packaged cherry tomatoes with pure PP were stored at 23 °C for 15 days, their headspace atmosphere experienced a rapid depletion of O_2 (7.0%) and an accumulation of CO_2 (6.1%). However, the concentration levels of O_2 and CO_2 of the PP/OD (83:17) composite film and the MP33000 film were maintained at atmospheric values over 15 days of storage; these results were similar to those with storage conditions at 9 °C. According to these results, all of packaged cherry tomatoes stored at lower temperatures (9 °C) exhibited relatively low respiration rates. When the temperature was 23 °C, however, the headspace atmosphere in the packaging prepared with the PP/OD (83:17) composite film and the MP33000 film exhibited a relatively lower depletion of O_2 and an accumulation of CO_2 compared to pure PP. In addition, the headspace atmosphere in the packaging with the PP/OD (83:17) composite film showed a lower CO_2 concentration than the MP33000 films, although the PP/OD (83:17) composite films were not perforated. According to the DSC, OTR, and WVTR results, this might have been because the PP/OD (83:17) composite film underwent a phase transition from the glassy state to the amorphous state when the temperature increased from 9 to 23 °C. During this temperature increase, the PP/OD (83:17) composite films seemed to open efficient diffusion paths for O_2 and CO_2; this positively contributed to the control of the headspace atmosphere in the packaging.

The firmness of cherry tomatoes is important for evaluating their freshness.[20,39,40] In general, the firmness of cherry tomatoes decreases during storage because metabolic changes induced by enzyme action and respiration soften their tissue.[20] As shown in Figure 9(a), the firmness of the cherry tomatoes packaged with the pure PP and MP33000 film at 9 °C decreased from 12.5 to 3.4 N and from 12.5 to 1.8 N, respectively. In addition, the firmness of the packaged cherry tomatoes with the PP/OD (83:17) composite film similarly decreased from 12.5 to 3.4 N. Thus, there was no significant difference in the deterioration rate among the different packaged cherry tomatoes at 9 °C. However, the firmness of cherry tomatoes packaged with the

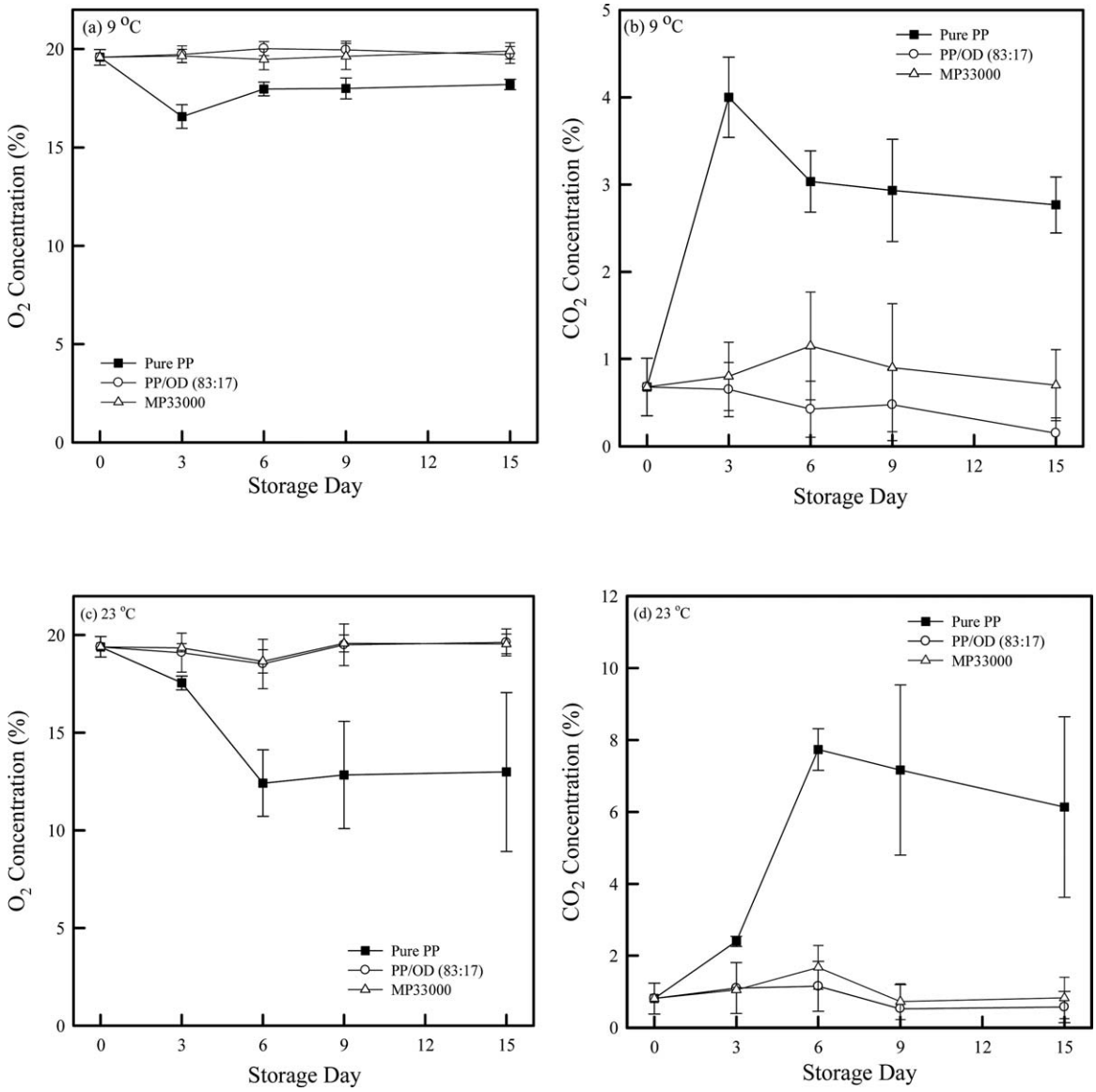

Figure 8. Changes in the O_2 and CO_2 concentrations of the headspace in packaging with the pure PP, a PP/OD (83:17) composite film, and an MP33000 film during storage at 9 and 23 °C.

pure PP film and MP33000 film decreased rapidly at 23 °C from 7.3 to 3.3 N and from 7.3 to 4.8 N, respectively, because of the rapid maturity. In contrast, the PP/OD (83:17) composite film led to a lower decrease in firmness from 7.3 to 5.2 N [Figure 9(b)]. Our results indicate that the PP/OD (83:17) composite films significantly reduced the firmness losses and delayed the deterioration rate of cherry tomatoes during storage at 23 °C; this could be attributed to the lower O_2 consumption and CO_2 accumulation in the headspace.

Color changes in cherry tomato skins are also a significant indication of ripening.[20,38] In the case of cherry tomato ripening, chlorophyll degrades from green to a colorless compound, and subsequently, carotenoids are synthesized from the colorless compound (phytoene) to form carotene (pale yellow), lycopene (red), and β-carotene (orange).[39,41] After 15 days of storage, the red/green (a^*) value of cherry tomatoes packaged with the pure PP and MP33000 films stored at 9 °C increased from 24.4 to 26.8 and from 24.4 to 26.2, respectively. The a^* value of the cherry tomatoes packaged with the PP/OD (83:17) composite film also increased slightly from 24.4 to 25.3 over 15 days of storage (Table IV). According to these results, there was no significant color change among the different packaged cherry tomatoes at 9 °C (Table IV). After 15 days of storage at 23 °C, the a^* values of the cherry tomatoes packaged with the pure PP and MP33000 film increased from 24.0 to 28.5 and from 24.0 to 29.5, respectively, because of the rapid maturity. In contrast, the change in the a^* value of the cherry tomatoes packaged with the PP/OD (83:17) composite film increased to a lesser extent from 24.0 to 27.8 (Table IV).

The respiration of products, gas permeabilities of the packaging material, and temperature change are considered significant factors affecting the quality of cherry tomatoes. The change in the

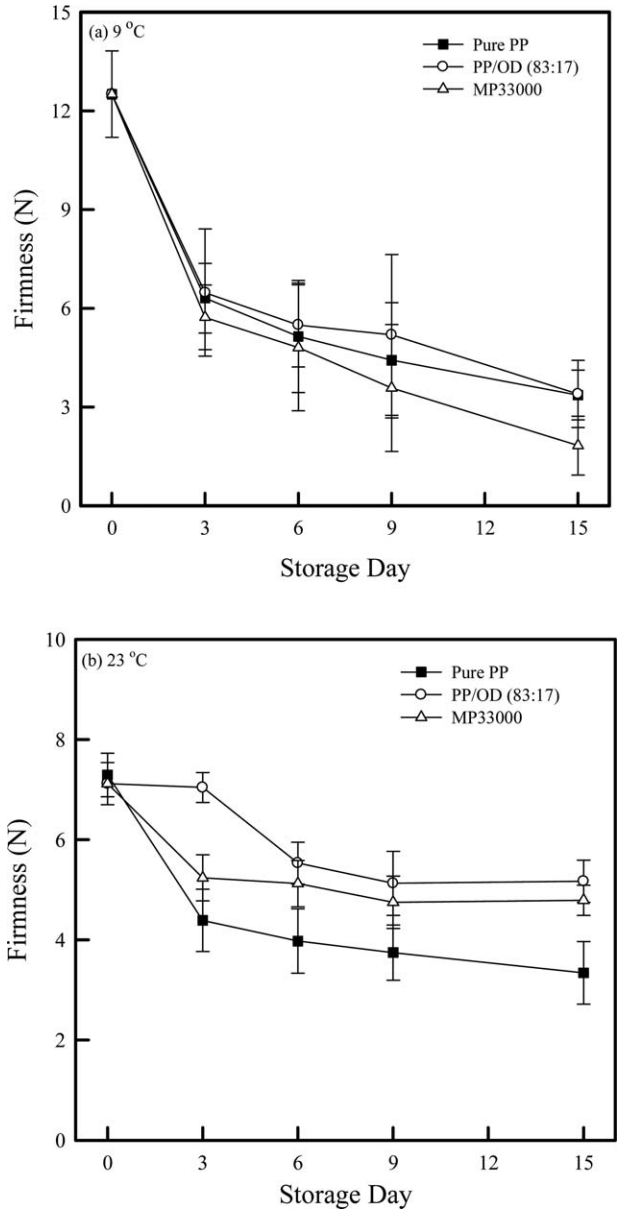

Figure 9. Changes in the firmness of cherry tomatoes packaged in a pure PP film, a PP/OD (83:17) composite film, and an MP33000 film during storage at (a) 9 and (b) 23 °C.

softening and color of cherry tomatoes is related to enzymatic activity originating from the gas concentration by respiration.[20,40] Compared to the pure PP, MP33000 films with constant gas permeabilities can control the gas concentrations in the headspace at constant levels at 9 and 23 °C. However, completely perforated systems may not protect against environmental factors (temperature, relative humidity, gas, and microorganisms), and this negatively affect the quality of the products. As shown by the SEM, DSC, OTR, and WVTR analyses, the oxygen and water vapor permeabilities of the PP/OD (83:17) composite film changed significantly with temperature, although it was a completely closed system. The composite film controlled the gas concentrations of the headspace at constant levels for safe storage and quality retention at 9 and 23 °C; this

Table IV. Color Index Values of the Cherry Tomatoes Packaged in the Pure PP Film, PP/OD (83:17) Composite Film, and MP33000 Film during Storage at 9 and 23 °C

	9 °C								23 °C							
	Pure PP			PP/OD (83:17)			MP33000		Pure PP			PP/OD (83:17)			MP33000	
Storage time (days)	L^*	a^*	b^*	L^*	a^*	b^*	L^*	a^*	b^*	L^*	a^*	b^*	L^*	a^*	b^*	L^*	a^*	b^*
0	35.4	24.4	21.9	35.4	24.4	21.9	35.4	24.4	21.9	40.5	24.0	24.4	40.5	24.0	24.4	40.5	24.0	24.4
3	33.8	25.1	20.8	34.2	24.6	19.9	35.2	24.6	20.2	39.6	26.0	23.2	38.7	26.0	22.2	38.1	25.8	23.2
6	34.7	25.1	20.0	34.3	25.4	20.1	35.9	25.4	21.9	38.0	26.0	22.1	38.1	25.9	20.5	37.5	26.9	21.6
9	34.9	25.5	20.9	35.3	25.2	18.9	35.1	26.5	20.8	38.7	26.6	22.8	37.3	26.5	19.6	38.0	27.0	20.8
15	34.1	26.8	19.4	34.8	25.3	19.3	35.2	26.2	21.6	39.4	28.5	22.8	38.0	27.8	19.9	37.9	29.5	21.3

L^*, lightness; b^*, yellow/blue.

prevented rapid enzymatic activities and could minimize the effects of environmental factors (temperature, relative humidity, gas, and microorganisms) on the quality of the products.

CONCLUSIONS

A series of PP/OD composite films were prepared with a twin-screw extruder. Their chemical, morphological, thermal, and surface properties and oxygen and water vapor permeabilities were characterized, and a storage test with cherry tomatoes was performed. The chemical and morphological structures of the PP/OD composite films were modified by the addition of OD, where the OD phase acted as a diffusion path for temperature-dependent oxygen and water vapor permeation. When the temperature was increased to be close to the phase-change temperature of OD, the segmental mobility of the OD phase started to increase, and its crystalline structure was converted to an amorphous structure. At a low concentration of OD, the permeation increase of the PP/OD composite films was relatively weak with increasing temperature. As the OD content increased, however, the oxygen and water vapor permeabilities of the composite films increased significantly with increasing temperature. During the phase-change process of OD in the PP matrix, the intramolecular interactions and crystallinity of OD in the PP decreased rapidly; this created permeation channels for oxygen and water vapor molecules in the PP matrix. In the storage test of the cherry tomatoes, the PP/OD (83:17) composite film effectively controlled the gas concentration of the headspace at 9 and 23 °C; this positively affected the firmness and color (a^* value) of the cherry tomatoes compared to the case when the pure PP and commercial MP33000 films were used as packaging films. According to these results, the increase in the temperature-dependent oxygen and water vapor permeation could be modified by the combination of PCMs with polymers. These can be used as an active packaging materials for preserving the quality and prolonging the shelf life of food and agricultural products by controlling their environmental conditions.

ACKNOWLEDGMENTS

This research was supported by the Basic Science Research Program through the National Research Foundation of Korea, which is funded by the Ministry of Education (contract grant number 2013R1A1A2057674), and by the Leaders Industry–University Cooperation Project, which is supported by the Ministry of Education of Korea.

REFERENCES

1. Chen, Y.; Liu, Y.; Fan, H.; Li, H.; Shi, B.; Zhou, H.; Peng, B. *J. Membr. Sci.* **2007**, *287*, 192.
2. Fuciños, C.; Fuciños, P.; Míguez, M.; Katime, I.; Pastrana, L. M.; Rúa, M. *L. PLOS One* **2014**, *9*, 1.
3. Kim, D.; Park, I.; Seo, J.; Han, H.; Jang, W. *J. Polym. Res.* **2015**, *22*, 1.
4. Lue, S. J.; Hsu, J.; Chen, C.; Chen, B. *J. Membr. Sci.* **2007**, *301*, 142.
5. Manolopoulou, H.; Lambrinos, G. R.; Chatzis, E.; Xanthopoulos, G.; Aravantinos, E. *J. Food Qual.* **2010**, *33*, 317.
6. O'Leary, K. A.; Paul, D. R. *Polymer* **2006**, *47*, 1226.
7. Hussein, Z.; Caleb, O. J.; Opara, U. L. *Food Packag. Shelf Life* **2015**, *6*, 7.
8. Winotapun, C.; Kerddonfag, N.; Kumsang, P.; Hararak, B.; Chonhenchob, V.; Yamwong, T.; Chinsirikul, W. *Packag. Technol. Sci.* **2015**, *28*, 367.
9. O'Leary, K. A.; Paul, D. R. *Polymer* **2006**, *47*, 1245.
10. Zhang, H.; Wang, X.; Wu, D. *J. Colloid Interface Sci.* **2010**, *343*, 246.
11. Zhang, Z.; Shi, G.; Wang, S.; Fang, X.; Liu, X. *Renewable Energy* **2013**, *50*, 670.
12. Salunkhe, P. B.; Shembekar, P. S. *Renewable Sustainable Energy Rev.* **2012**, *16*, 5603.
13. Chen, F.; Wolcott, M. P. *Eur. Polym. J.* **2014**, *52*, 44.
14. Krupa, I.; Luyt, A. S. *Thermochim. Acta* **2001**, *372*, 137.
15. Molefi, J. A.; Luyt, A. S.; Krupa, I. *Thermochim. Acta* **2010**, *500*, 88.
16. Cai, Q.; Xu, R.; Chen, X.; Chen, C.; Mo, H.; Lei, C. *Polym. Compos.* **2015**, DOI: 10.1002/pc.23462.
17. Shimizu, R. N.; Demarquette, N. R. *J. Appl. Polym. Sci.* **2000**, *76*, 1831.
18. Khayet, M.; Chowdhury, G.; Matsuura, T. *AIChE J.* **2002**, *48*, 2833.
19. Khayet, M.; Fernáadez, V. *Theor. Biol. Med. Model.* **2012**, *9*, 1.
20. Choi, D. S.; Park, S. H.; Choi, S. R.; Kim, J. S.; Chun, H. H. Food Packag. *Shelf Life* **2015**, *3*, 19.
21. Xiao, Z.; Luo, Y.; Lester, G. E.; Kou, L.; Yang, T.; Wang, Q. *LWT Food Sci. Technol.* **2014**, *55*, 551.
22. García-García, I.; Taboada-Rodríguez, A.; Marín-Iniesta, F. *Food Bioprocess Technol.* **2013**, *6*, 754.
23. Sevegney, M. S.; Kannan, R. M.; Siedle, A. R.; Percha, P. A. *J. Polym. Sci. Part B: Polym. Phys.* **2005**, *43*, 439.
24. Urbaniak-Domagala, W. In Advanced Aspects of Spectroscopy; Farrukh, M. A., Ed.; InTech: Rijeka, Croatia, **2012**; Chapter 3, p *85*.
25. Chung, O.; Jeong, S.-G.; Kim, S. *Sol. Energy Mater. Sol. Cells* **2015**, *137*, 107.
26. Li, H.; Liu, X.; Fang, G.-Y. *Appl. Phys. A* **2010**, *100*, 1143.
27. Jawalar, S. S.; Aminabhavi, T. M. *Polymer* **2006**, *47*, 8061.
28. Qiu, X.; Song, G.; Chu, X.; Li, X.; Tang, G. *Thermochim. Acta* **2013**, *551*, 136.
29. Li, W.; Song, G.; Tang, G.; Chu, X.; Ma, S.; Liu, C. *Energy* **2011**, *36*, 785.
30. Shan, X. L.; Wang, J. P.; Zhang, X. X.; Wang, X. C. *Thermochim. Acta* **2009**, *494*, 104.
31. Jakab, E.; Várhegyi, G.; Faix, O. *J. Anal. Appl. Pyrol.* **2000**, *56*, 273.
32. Beyler, C. L.; Hirschler, M. M. In SFPE Handbook of Fire Protection Engineering, 4th ed.; Dinenno, P. J., Drysdale, D.,

Beyler, C. L., Walton, W. D., Eds.; Springer: New York, **2002**; Chapter 7, p 110.

33. Alavi, S.; Thomas, S.; Sandeep, K. P.; Kalarikkal, N.; Varghese, J.; Yaragalla, S. Polymers for Packaging Applications; Apple Academic: Toronto, **2015**; pp 3 and 405.
34. Kirkland, B. S.; Paul, D. R. *Polymer* **2008**, *49*, 507.
35. Trigui, A.; Karkri, M.; Krupa, I. *Energy Conversion Manage.* **2014**, *77*, 586.
36. Michaels, A.; Bixler, H. J. *J. Polym. Sci. Polym. Chem. Ed.* **1961**, *50*, 413.
37. Mogri, Z.; Paul, D. R. *Polymer* **2001**, *42*, 7765.
38. Michalski, M.-C.; Hardy, J.; Saramago, B. J. V. *J. Colloid Interface Sci.* **1998**, *208*, 319.
39. Bailén, G.; Guillén, F.; Castillo, S.; Serrano, M.; Valero, D.; Martínez-Romero, D. *J. Agric. Food. Chem.* **2006**, *54*, 2229.
40. Islam, M. Z.; Kim, Y. S.; Kang, H.-M. *J. Bio-Environ. Control* **2011**, *20*, 221.
41. Giuliano, G.; Bartley, G. E.; Scolnik, P. A. *Plant Cell* **1993**, *5*, 379.